Marked variation in atherosclerotic plaque progression between the major epicardial coronary arteries

Bax, A.M.; Lin, F.Y.; Rosendael, A.R. van; Ma, X.Y.; Lu, Y.; Hoogen, I.J. van den; ... ; PARADIGM Investigators

ESC European Society of Cardiology

European Heart Journal - Cardiovascular Imaging (2022) **23**, 1482–1491
https://doi.org/10.1093/ehjci/jeac044

ORIGINAL PAPER

Marked variation in atherosclerotic plaque progression between the major epicardial coronary arteries

A. Maxim Bax[1], Fay Y. Lin[1], Alexander R. van Rosendael[2], Xiaoyue Ma[3], Yao Lu[3], Inge J. van den Hoogen[2], Umberto Gianni[1], Sara W. Tantawy[1], Daniele Andreini[4], Matthew J. Budoff[5], Filippo Cademartiri[6], Kavitha Chinnaiyan[7], Jung Hyun Choi[8], Edoardo Conte[4], Pedro de Araújo Gonçalves[9], Ilan Gottlieb[10], Martin Hadamitzky[11], Jonathon A. Leipsic[12], Erica Maffei[13], Gianluca Pontone[4], Gregg Stone[14], Sanghoon Shin[15], Yong-Jin Kim[16], Byoung Kwon Lee[17], Eun Ju Chun[18], Ji Min Sung[19,20], Sang-Eun Lee[15,20], Daniel S. Berman[21], Jagat Narula[22], Hyuk-Jae Chang[19,20], and Leslee J. Shaw[1]*, for the PARADIGM Investigators

[1]Department of Radiology, Dalio Institute of Cardiovascular Imaging, NewYork-Presbyterian Hospital and Weill Cornell Medicine, 413 East 69th Street, Suite 108, New York, NY 10021, USA; [2]Department of Cardiology, Leiden University Medical Center, Leiden, The Netherlands; [3]Department of Healthcare Policy and Research, NewYork-Presbyterian Hospital and the Weill Cornell Medical College, New York, NY, USA; [4]Department of Perioperative Cardiology and Cardiovascular Imaging, Centro Cardiologico Monzino IRCCS, Milan, Italy; [5]Department of Medicine, Los Angeles Biomedical Research Institute, Torrance, CA, USA; [6]Department of Radiology, Fondazione Monasterio-CNR (FTGM), Pisa, Italy; [7]Department of Cardiology, William Beaumont Hospital, Royal Oak, MI, USA; [8]Division of Cardiology, Department of Internal Medicine, Pusan University Hospital, Busan, South Korea; [9]Departmento of Cardiology, UNICA, Unit of Cardiovascular Imaging, Hospital da Luz, Lisboa, Portugal; [10]Department of Radiology, Casa de Saude São Jose, Rio de Janeiro, Brazil; [11]Department of Radiology and Nuclear Medicine, German Heart Center Munich, Munich, Germany; [12]Department of Medicine and Radiology, University of British Columbia, Vancouver, BC, Canada; [13]Department of Radiology, Area Vasta 1/ASUR Marche, Urbino, Italy; [14]The Zena and Michael A. Wiener Cardiovascular Institute, Icahn School of Medicine at Mount Sinai, New York, NY, USA; [15]Division of Cardiology, Department of Internal Medicine, Ewha Womans University Seoul Hospital, Seoul, Korea; [16]Department of Internal Medicine, Seoul National University College of Medicine, Cardiovascular Center, Seoul National University Hospital, Seoul, South Korea; [17]Division of Cardiology, Department of Internal Medicine, Gangnam Severance Hospital, Yonsei University College of Medicine, Seoul, Korea; [18]Department of Radiology, Seoul National University Bundang Hospital, Sungnam, South Korea; [19]Division of Cardiology, Severance Cardiovascular Hospital, Yonsei University College of Medicine, Yonsei University Health System, Seoul, South Korea; [20]Yonsei-Cedars-Sinai Integrative Cardiovascular Imaging Research Center, Yonsei University College of Medicine, Yonsei University Health System, Seoul, South Korea; [21]Department of Imaging and Medicine, Cedars Sinai Medical Center, Los Angeles, CA, USA; and [22]Department of cardiology, Icahn School of Medicine at Mount Sinai, Mount Sinai Heart, Zena and Michael A. Wiener Cardiovascular Institute, and Marie-Josée and Henry R. Kravis Center for Cardiovascular Health, New York, NY, USA

Received 29 May 2021; editorial decision 10 January 2022; online publish-ahead-of-print 26 April 2022

Aims Atherosclerosis develops progressively and worsens over time, yet event risk patterns vary in the left circumflex (LCx), right coronary artery (RCA) and left anterior descending (LAD). The aim of this analysis was to examine varying progressive disease alterations between the three major coronary arteries.

Methods and results Patients were included from a prospective, international registry of consecutive patients who underwent serial CCTA at a median interval of 3.3 years. Annual progression of quantitative total and compositional plaque volume were compared between the three coronary arteries (LCx, LAD, and RCA). Other analyses compared stenosis ≥50% and new high-risk plaque (HRP; ≥2 of the following: spotty calcification, positive remodelling, napkin-ring sign, and low-attenuation plaque) on follow-up. Generalized estimating equations and marginal Cox regression models were used to compare progression, with covariate adjustment by the baseline atherosclerotic cardiovascular disease risk score, statin use, and plaque burden. Quantitative plaque measurements were calculated in 1344 patients (age 60 ± 9 years, 57% men). Plaque progression occurred less often in the LCx (41.0%) as compared to the RCA (52.7%) and LAD (77.4%, $P < 0.001$). Odds for annual plaque burden increase ≥population mean were 1.98- and 1.43-fold as high in the LAD ($P < 0.001$) and RCA ($P < 0.001$) as compared to the LCx. Similarly, the LAD

* Corresponding author. Tel: +1 404 518 3021. E-mail: les2035@med.cornell.edu

was associated with a 2.45 higher risk of progression to obstructive CAD ($P < 0.001$), as compared to the LCx; with no differences between the RCA and LCx ($P = 0.13$). New HRP lesions formed least often in the LCx (3.4%), followed by the RCA (8.1%) and most often in the LAD (10.1%; $P < 0.001$).

Conclusions Our findings reveal novel insights into varied patterns of atherosclerotic plaque progression within the LCx as compared to the other epicardial coronary arteries. These varied patterns reflect differing stages in the disease process or differing pathogenic milieu across the coronary arteries.

Graphical Abstract

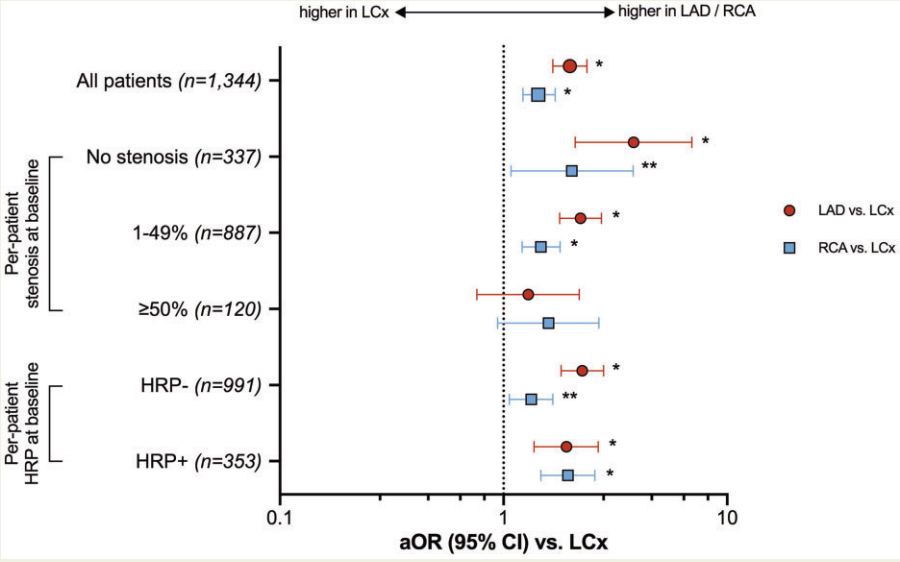

Keywords atherosclerosis • coronary computed tomography angiography • plaque progression

Introduction

Atherosclerosis develops progressively and worsens over time in terms of the burden and diffusivity of plaque and stenosis severity. The most common clinical indicator to examine atherosclerotic plaque progression is when a patient with known coronary artery disease (CAD) presents with a morbid or fatal coronary event.[1–3] The majority of this evidence supports that patients with more severe and extensive atherosclerotic plaque have a higher risk of major CAD events and that specific high-risk plaque (HRP) features, such as positive remodelling or low attenuation plaque, further delineate adverse event risk.[1,3,4] To date, however, the evidence is minimal as to specific patterns of progressive disease that may be documented with serial anatomic testing. Earlier evidence using intravascular ultrasound in higher risk patients often compared the effect of lipid-lowering therapies on atherosclerotic plaque regression.[5] These trials and related observational series have focused on morphologic and dimensional changes following intervention and largely examined near-term interval differences reflective of advancing or improved disease states. Within the current evidence, specific signatures of variable plaque progression have yet to be defined, specifically those observed in lower risk patients presenting with suspected CAD undergoing serial coronary computed tomographic angiography (CCTA).

Importantly, data are often pooled across the major coronary arteries when determining progressive alterations. Measurement of progression largely assumes uniformity in plaque growth across the epicardial coronary tree. Variability in atherosclerotic plaque alterations by vessel and disease burden has dramatic implications for the evaluation of symptomatic patients referred to anatomic testing; especially in terms of expected progressive disease states and risk of acute coronary syndromes. Our group has recently reported on differences between the major epicardial coronary arteries [i.e. left circumflex (LCx) vs. right coronary artery (RCA) and left anterior descending (LAD)] based on CCTA measures of atherosclerotic plaque volume, stenosis severity, and HRP features.[6] We reported a lower overall plaque burden in the LCx when compared with the LAD and RCA. In this report, we extend these prior findings by examining signature patterns of atherosclerotic plaque progression

across the three major coronary arteries. Thus, the aim of this analysis was to examine the extent to which baseline differences impart varying progressive disease risk including alterations in high-risk atherosclerotic plaque features and worsening stenosis severity.

Methods

Study design and patient population

The Progression of AtheRosclerotic PlAque DetermIned by Computed TomoGraphic Angiography Imaging (PARADIGM) study is a dynamic, international, multicentre observational registry designed to monitor changes in atherosclerosis on CCTA.[7] A total of 2252 consecutive patients were consecutively enrolled in a registry where each participant underwent clinically indicated serial CCTA with an interscan-interval of ≥2 years were enrolled. Exclusion criteria included prior myocardial infarction or coronary revascularization prior to the baseline CCTA ($n = 282$), an uninterpretable CCTA for quantification ($n = 492$), and intercurrent CAD event or coronary revascularization before the follow-up CCTA ($n = 133$). Thus, for this report, the final study population consisted of 1344 patients. All enrolment procedures and research methods were approved by each centre's institutional review board.

Site CCTA protocol and core laboratory image interpretation

We have previously reported, in detail, methods regarding CCTA image acquisition at the participating sites.[8] In brief, all CCTAs were performed in accordance with the Society of Cardiovascular Computed Tomography guidelines.[9] Datasets from each participating site were transferred to a core laboratory for blinded image analysis.

At the CCTA Core Laboratory, image interpretation was completed by Level III certified physicians using quantitative plaque software (QAngioCT Research Edition v2.1.9.1, Medis Medical Imaging Systems, Leiden, the Netherlands).[10] Details on the quantification methodology have previously been reported.[8] All coronary arteries and their branches with a diameter ≥2 mm were evaluated according to a modified 17-segment American Heart Association model. Presence of plaque was defined as any tissue ≥1 mm^2 identified in >2 planes, within or adjacent to the lumen that could be discriminated from surrounding structures and the lumen.[11] For longitudinal comparisons, coronary segments and lesions were co-registered between baseline and follow-up CCTA, using fiduciary landmarks, such as coronary artery side branches.

Plaque volume (mm^3) and vessel volume (mm^3) were quantified for all coronary segments and summed to generate vessel-level data. Plaque volume was categorized according to composition, using predefined Hounsfield Unit (HU) thresholds, into necrotic core (-30 to 30 HU), fibrofatty (31–130 HU), fibrous (131–350 HU), and calcified plaque (>350 HU).[12,13] Due to the small volume of necrotic core (mean volume: 0.8 ± 3.6 mm^3), we merged necrotic core with fibrofatty plaque (and this will be referred to as 'necrotic core and fibrofatty plaque combined'). Percent atheroma volume (PAV) was defined as [(plaque volume/vessel volume) × 100].[14] Furthermore, presence of CAD was evaluated in each coronary artery, using a cut-off value of ≥50% stenosis for obstructive CAD.[15] The presence of HRP was defined as coronary lesions with ≥2 of the following features: spotty calcification, low-attenuation plaque, napkin-ring sign, and positive remodelling, as previously described.[16,17] Annual changes in plaque volume (Δplaque volume/year; mm^3/year) and PAV (ΔPAV/year; %/year) were calculated by subtracting values at baseline from follow-up and dividing the result by the CCTA interval time.

Study endpoints

The primary comparison examined annual changes in plaque volume (both total and per compositional subtype) and PAV. Also, prompt annualized progression was defined as ΔPAV/year >0.57%, based on prior work completed by our group.[18,19] Secondary analyses examined prompt annualized plaque progression using the median PAV/year as a cut-off. In addition to prompt plaque progression, we examined progression to obstructive CAD at follow-up among vessels with no- or non-obstructive CAD on the baseline CCTA.[19]

Statistical methods

Continuous variables are presented as mean ± standard deviation (SD) or median with quartiles (Q1–Q3), categorical variables are presented as absolute numbers and percentages. Continuous variables were compared using Friedman test or Wilcoxon signed-rank test, as appropriate. Categorical variables were compared using the χ^2 test or Fisher's exact test. Logistic generalized estimating equations (GEE) models were used to calculate odds for prompt plaque progression across the coronary arteries. Furthermore, a subset of vessels without obstructive CAD at baseline were analysed to predict progression to obstructive CAD at follow-up. Marginal Cox models with multivariate failure times were used to account for within-patient clustering of the data. Both models were adjusted for the AtheroSclerotic CardioVascular Disease (ASCVD) risk score, statin use and per-vessel PAV at baseline. Results are presented as adjusted odds ratios (aORs) or adjusted hazard ratios (aHRs) along with 95% confidence intervals (CI). Two-tailed *P*-values of <0.05 were considered statistically significant. All analyses were performed in SAS version 9.4 (SAS Institute, Inc., Cary, NC, USA) and SPSS Statistics version 26 (IBM Corporation, Armonk, NY, USA).

Results

Clinical history and stress test findings

Of the 1344 patients, the mean age of the patients at baseline was 60.4 ± 9.4 years, with 57% being male (*Table 1*). Most patients were referred for evaluation of anginal symptoms for the baseline CCTA. The average enrolled patient had an intermediate ASCVD risk score and slightly more than one-third of patients were on statin therapy at baseline.

Patients underwent follow-up CCTA after a median interval time of 3.3 (2.6–4.8) years. *Table 1* also reports clinical risk factor data collected at the time of the follow-up CCTA. As patients were older at the time of their second CCTA, increases in the ASCVD risk score were reported. The follow-up utilization of statin therapy was much higher than that reported at baseline (56.6% vs. 39.8%).

Quantitative atherosclerotic plaque progression

Quantitative plaque analysis was performed at baseline and follow-up CCTA (*Table 2*). Plaque volume at baseline[6] was smallest in the LCx (10.2 ± 30.5 mm^3), followed by the RCA (33.5 ± 86.2 mm^3; $P < 0.001$) and the LAD (58.3 ± 85.3 mm^3; $P < 0.001$). Similar findings were noted for PAV (LCx: 2.1 ± 5.4% vs. RCA: 2.9 ± 6.4% vs. LAD: 6.4 ± 8.3%; both $P < 0.001$). The volume of plaque compositional subtypes (necrotic core and fibrofatty plaque, fibrous plaque, and calcified plaque) were also lowest in the LCx ($P < 0.001$ compared to LAD and RCA).

Table 1 Clinical characteristics of the 1344 patients with a baseline and ≥2-year follow-up CCTA

	Baseline CCTA	Follow-up CCTA[a]
Age, mean ± SD (years)	60.4 ± 9.4	64.2 ± 9.5
BMI, mean ± SD (kg/m^2)	25.4 ± 3.4	25.5 ± 3.4
ASCVD risk score, median (IQR) (%)	9.5% (4.6–18.0%)	12.3% (6.1–23.4%)
Anginal symptoms (%)	84.7	81.0
Risk factor measurement		
SBP/DBP (mmHg)	130/80	126/77
Total cholesterol (mg/dL)	190.3 ± 39.0	174.1 ± 37.6
LDL cholesterol (mg/dL)	115.7 ± 33.8	102.1 ± 32.7
Triglycerides (mg/dL)	144.4 ± 87.0	132.4 ± 80.3
Glucose (mg/dL)	107.6 ± 31.6	108.0 ± 27.1
Statin medication use (%)	39.8	56.6

ASCVD, atherosclerotic cardiovascular disease; BMI, body mass index; CCTA, coronary computed tomographic angiography; DBP, diastolic blood pressure; IQR; inter-quartile range; LDL, low-density lipoprotein; SBP, systolic blood pressure.
[a]Follow-up CCTA was performed a median of 3.3 (2.6–4.8) years after the baseline CCTA.

Table 2 Baseline and progressive changes in atherosclerotic plaque volume between the three major coronary arteries

	LCx (n = 1297)	LAD (n = 1334)	RCA (n = 1300)	*P* value		
				Overall[a]	LCx vs. LAD[b]	LCx vs. RCA[b]
Baseline CCTA						
Vessel length (mm)	99.2 ± 47.1	165.5 ± 59.5	150.9 ± 53.5	<0.001	<0.001	<0.001
Vessel volume (mm^3)	478.6 ± 317.0	883.1 ± 404.8	1033.0 ± 617.8	<0.001	<0.001	<0.001
Plaque volume (mm^3)	10.2 ± 30.5	58.3 ± 85.3	33.5 ± 86.2	<0.001	<0.001	<0.001
Necrotic core and fibrofatty (-30 to 130 HU)	1.2 ± 5.8	12.8 ± 27.5	6.3 ± 20.1	<0.001	<0.001	<0.001
Fibrous (131–350 HU)	4.8 ± 15.2	24.7 ± 36.5	15.7 ± 41.3	<0.001	<0.001	<0.001
Calcified (>350 HU)	4.2 ± 14.8	20.9 ± 45.5	11.6 ± 42.0	<0.001	<0.001	<0.001
PAV (%)	2.1 ± 5.4	6.4 ± 8.3	2.9 ± 6.4	<0.001	<0.001	<0.001
Atherosclerotic plaque progression						
Any plaque progression (Δ volume >0)	532 (41.0%)	1032 (77.4%)	685 (52.7%)	<0.001		
Annualized Δ in plaque volume (mm^3/year)	1.8 ± 4.4	7.3 ± 11.6	6.4 ± 14.5	<0.001	<0.001	<0.001
Necrotic core and fibrofatty (-30 to 130 HU)	0.0 ± 1.4	0.5 ± 6.0	0.7 ± 6.5	0.090	0.998	0.023
Fibrous (131–350 HU)	0.5 ± 2.5	2.5 ± 7.4	2.4 ± 8.2	<0.001	<0.001	<0.001
Calcified (>350 HU)	1.3 ± 3.6	4.3 ± 7.2	3.3 ± 8.7	<0.001	<0.001	<0.001
ΔPAV/year (%/year)	0.4 ± 0.9	0.8 ± 1.2	0.6 ± 1.1	<0.001	<0.001	<0.001

Data are presented as mean ± standard deviation or as %.
CCTA, coronary computed tomography angiography; LAD, left anterior descending; LCx, left circumflex; RCA, right coronary artery; PAV, percent atheroma volume.
[a]Data are compared using a Friedman test.
[b]Data are compared using a Wilcoxon signed-rank test.

Plaque progression (defined as Δ plaque volume >0 mm^3) occurred less often in the LCx (41.0%), followed by the RCA (52.7%) while occurring most often in the LAD (77.4%; $P < 0.001$). Mean annualized plaque volume progression was lowest in the LCx (Δ plaque volume/year 1.8 ± 4.4 mm^3/year), compared to the RCA (6.4 ± 14.5 mm^3/year; $P < 0.001$) and LAD (7.3 ± 11.6 mm^3/year; $P < 0.001$). Annualized PAV progression was also lowest in the LCx (ΔPAV/year 0.4 ± 0.9%/year), followed by the RCA (0.6 ± 1.1%/year; $P < 0.001$) and highest in the LAD (0.8 ± 1.2%/year; $P < 0.001$). Furthermore, annualized progression of fibrous and calcified plaque volume was lowest in the LCx (all $P < 0.001$). The volume of necrotic core and fibrofatty plaque combined changed minimally over time in the LCx (0.0 ± 1.4 mm^3/year), while it was more variable but not statistically different in the LAD (0.5 ± 6.0 mm^3/year; $P > 0.9$; Supplementary data online, *Figure S1*). In the RCA, there was a statistical difference compared to the LCx (0.7 ± 6.5 mm^3/year; $P = 0.023$;

Table 3 Prevalence of HRP at baseline and newly identified on the follow-up CCTA between the three major coronary arteries

	LCx ($n = 1297$)	LAD ($n = 1334$)	RCA ($n = 1300$)	*P* value
Baseline CCTA				
HRP	40 (3.1%)	256 (19.2%)	130 (10.0%)	<0.001
Low attenuation plaque	22 (1.7%)	189 (14.2%)	91 (7.0%)	<0.001
Positive remodelling	298 (23.0%)	726 (54.4%)	428 (32.9%)	<0.001
Napkin ring sign	0 (0%)	8 (0.6%)	1 (0.1%)	0.003
Spotty calcification	34 (2.6%)	177 (13.3%)	81 (6.2%)	<0.001
New on follow-up CCTA				
HRP	44 (3.4%)	135 (10.1%)	105 (8.1%)	<0.001
Low attenuation plaque	12 (0.9%)	75 (5.6%)	53 (4.1%)	<0.001
Positive remodelling	219 (16.9%)	347 (26.0%)	318 (24.5%)	<0.001
Napkin ring sign	2 (0.2%)	1 (0.1%)	1 (0.1%)	0.70
Spotty calcification	35 (2.7%)	92 (6.9%)	71 (5.5%)	<0.001

Data are presented as frequencies (%).
CCTA, coronary computed tomography angiography; HRP, high-risk plaque; LAD, left anterior descending; LCx, left circumflex; RCA, right coronary artery.

Supplementary data online, *Figure S1*). Overall, similar results were noted when stratifying for sex (Supplementary data online, *Table S1*).

High-risk plaque features

On the baseline CCTA, the prevalence of HRP was lowest in the LCx (3.1%; *Table 3*), followed by the RCA (10.0%) and highest in the LAD (19.2%; $P < 0.001$). At baseline, specific HRP features were also least prevalent in the LCx ($P < 0.004$ for all). On the follow-up CCTA, new HRP were identified least often in the LCx (3.4%), followed by the RCA (8.1%) and most often in the LAD (10.1%; $P < 0.001$). Similar findings were noted by specific HRP features; except for the napkin-ring sign, which was noted in only a few patients ($P = 0.7$).

Prompt annualized atherosclerotic plaque progression

The aOR for prompt annualized progression was calculated using a logistic GEE model, adjusted for the baseline ASCVD risk, baseline statin use and baseline per-vessel PAV (*Figure 1* and Supplementary data online, *Table S2*). Overall, as compared to the LCx, prompt annualized plaque progression was more likely to occur in the LAD [OR 1.98 (95% CI: 1.66–2.36); $P < 0.001$] and RCA [OR 1.43 (95% CI: 1.22–1.70); $P < 0.001$]. Among patients with a normal CCTA at baseline, the aOR for prompt annualized plaque progression was similarly higher in the LAD (OR 3.82; $P < 0.001$) and RCA (OR 2.02; $P = 0.028$). Similar differences were revealed among patients with non-obstructive CAD at baseline (LAD OR 2.21 and RCA OR 1.47; both $P < 0.001$) as compared to the LCx. Higher aOR were also found when stratifying for the presence or absence of HRP at baseline in the LAD and RCA as compared to the LCx ($P < 0.05$). However, no differences were identified between the coronary arteries for patients with obstructive CAD at baseline ($P > 0.05$). Similar findings were noted when the median value for prompt plaque progression was applied to our population subgroup (Supplementary data online, *Table S3*).

Progression of stenosis severity

Figure 2 reports the prevalence of normal, non-obstructive CAD, and obstructive CAD at baseline and follow-up; with particular differences noted in non-obstructive CAD between the LCx as compared to the LAD and RCA ($P < 0.001$). We also employed a marginal Cox regression to estimate progression to obstructive CAD at follow-up among those whose baseline CCTA was normal or had non-obstructive CAD; including covariate adjustment by the baseline ASCVD risk score, statin use, and per-vessel PAV (*Figure 2*). When compared with the LCx, the LAD was associated with a higher risk of progression to obstructive CAD [aHR 2.45 (95% CI: 1.49-4.02); $P < 0.001$]; with no differences noted for the RCA [aHR 1.51 (95% CI: 0.89-2.56); $P = 0.13$].

Compositional changes in atherosclerotic plaque

As shown in *Figure 3*, plaque composition varied between the three major coronary arteries. At baseline, the proportion of total plaque volume consisting of necrotic core and fibrofatty plaque were smallest in the LCx [2.6% vs. 8.0% (RCA) and 11.1% (LAD); $P < 0.001$]; with these findings persisting on the follow-up CCTA ($P < 0.001$). Interestingly, on the baseline and follow-up CCTA, calcified plaque comprised the largest proportion of total plaque in the LCx at baseline [39.5% vs. 27.6% (LAD) and 28.0 (RCA); $P < 0.001$] and at follow-up [LCx: 52.7% vs. 40.1% (LAD) and 40.5% (RCA); $P < 0.001$]. On follow-up as compared to baseline, the proportion of non-calcified plaque had decreased in all coronary arteries ($P < 0.001$), whereas the proportion of

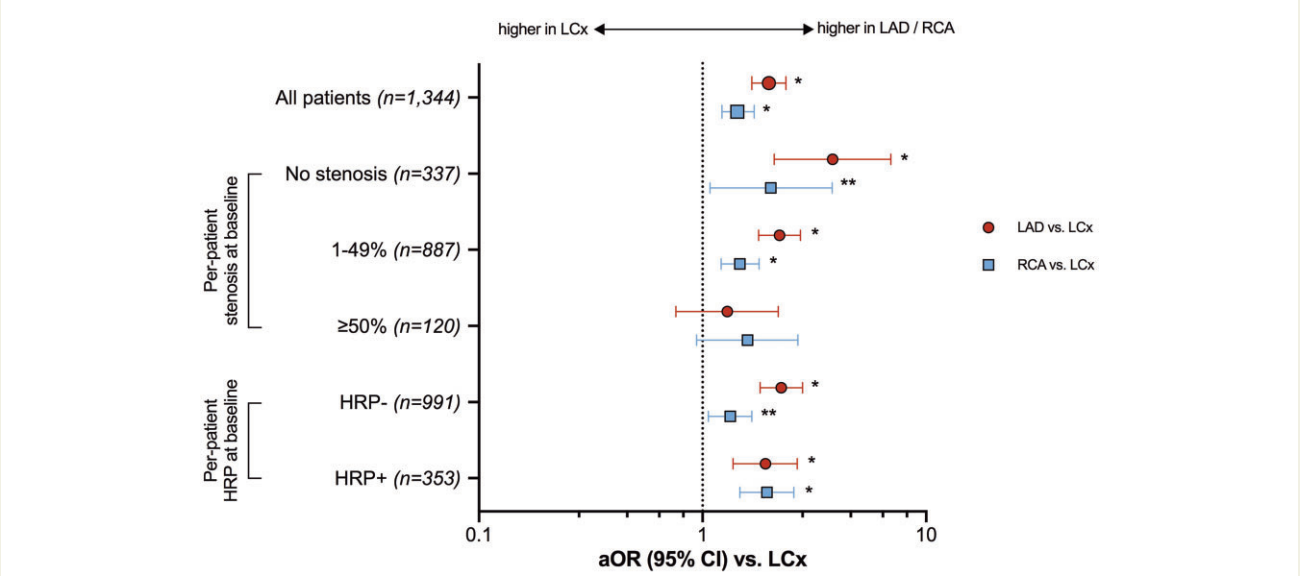

Figure 1 Adjusted odds ratios (aORs) for prompt plaque progression between the three major coronary arteries. Prompt plaque progression was defined as annual ΔPAV ≥0.57%/year. The aOR was calculated using a logistic GEE model, including the following covariates: baseline ASCVD risk score, statin use, and per-vessel PAV. The overall results are presented as well as stratified by baseline stenosis severity and HRP. *$P < 0.001$. **$P < 0.05$.

calcified plaque had increased ($P < 0.001$). When analysing statin taking and statin naïve patients separately, similar results were observed (Supplementary data online, *Table S4*).

Discussion

Among patients presenting for a diagnostic evaluation, most symptomatic patients have detectable coronary atherosclerosis and remain at risk for progressive CAD states.[20] In this report, we explored variability in patterns of atherosclerotic progression across the epicardial coronary arteries and report significantly lower rates of plaque progression in the LCx as compared to the LAD and RCA. These findings persisted in multivariable models ($P < 0.001$) even when adjusting for a variety of factors, such as statin use, the ASCVD risk score, and baseline plaque burden. In fact, progression to obstructive CAD occurred significantly less often in the LCx as compared to the LAD ($P < 0.001$). Moreover, new lesions with HRP (e.g. positive remodelling), associated with plaque vulnerability and ACS risk, were less likely to form in the LCx (3.4%) as compared to the LAD (10.1%) or RCA (8.1%). This pattern of less intensive changes in the LCx may reflect an earlier stage of CAD, given the lower burden of disease on the baseline CCTA. However, it may also reflect a differing pathogenic milieu between the coronary arteries and these findings clarify observed differences in terms of ACS risk; being lowest in the LCx and highest in the LAD.

Divergent pathways to disease progression

Our imaging perspective of visualizing the epicardial coronary arteries has largely been one of uniformity in detection of obstructive CAD and high-risk atherosclerotic plaque.[2,17] However, our analysis focuses on differences between the major epicardial coronary arteries and our findings impact diagnostic risk estimations and expected adverse sequelae following CCTA. We may define these differences using the term topography whereby graphical details and features may formulate varied patterns of atherosclerotic disease progression in the LCx as compared to the LAD and RCA. Although prior reports have defined a comprehensive CCTA interpretation based on CAD extent, severity, and composition,[21] we report a different pattern of atherosclerotic progression in the LCx respective to the other major epicardial arteries, with slower progression rates and higher proportions of calcified plaque on follow-up. The differences between coronary arteries noted at baseline could be a marker for the currently observed differences in plaque progression. There are a myriad of potential underlying pathophysiological mechanisms that could elicit differences in the progression of atherosclerotic plaque. Local variations in coronary anatomy (e.g. bifurcations and tortuosity) and haemodynamics (e.g. endothelial shear stress)[22,23] have been such suggested explanations for predisposition of coronary segments to atherogenesis.

Studies examining plaque characteristics using other imaging modalities or post-mortem histopathology have reported findings consistent with our results. Specifically, histopathological studies have shown an increased susceptibility to atherosclerosis in the LAD, especially its proximal segment.[24,25] On autopsy of 113 patients after sudden coronary death, Virmani *et al.*[26] found that thin-cap fibroatheroma lesions are predominantly located in the proximal and middle LAD (42%), followed by the proximal and middle RCA (20%) and proximal LCx (18%), and supported by similar series.[27] Moreover, results from three-vessel intravascular ultrasound, performed on 697

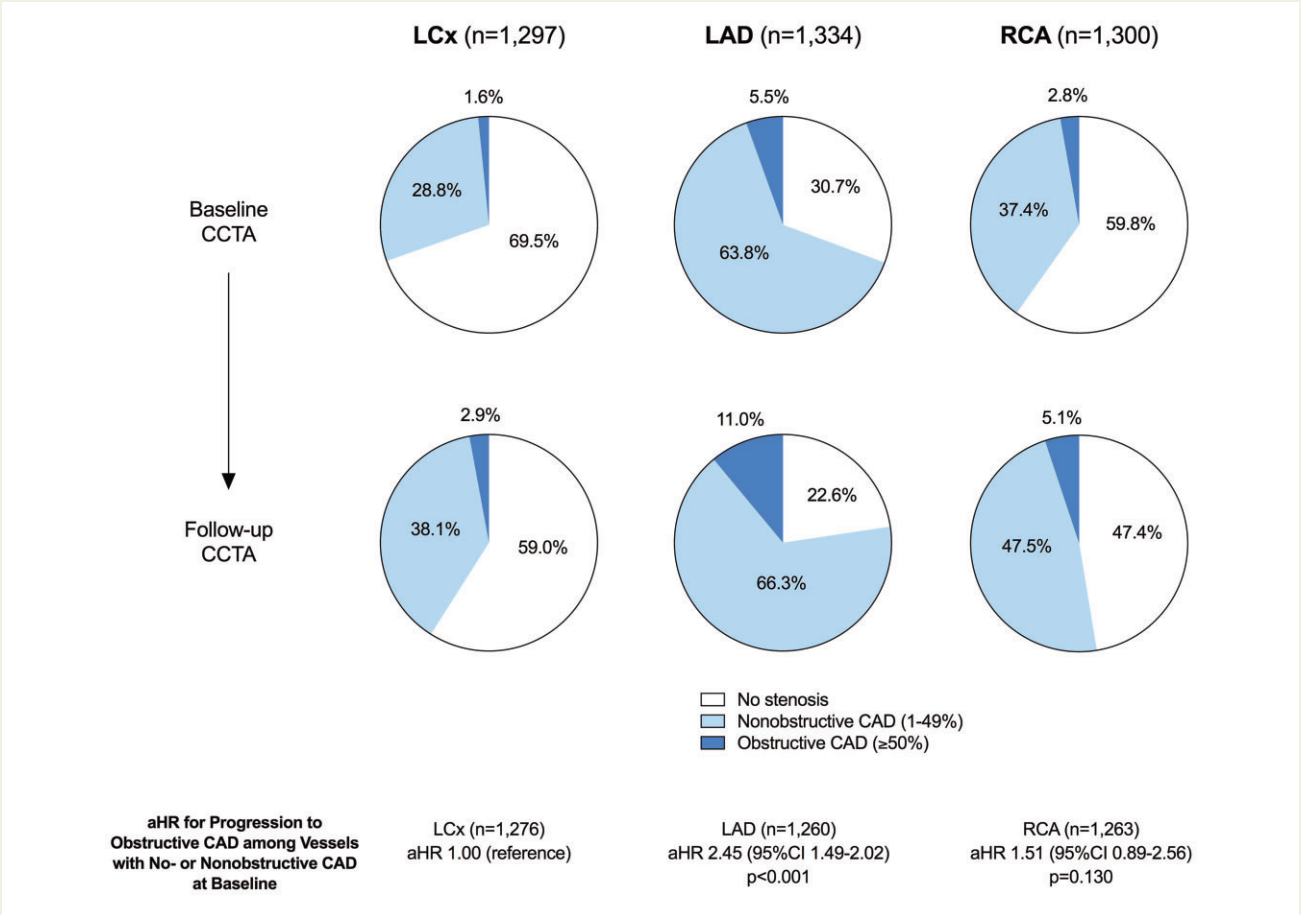

Figure 2 Baseline and follow-up CCTA stenosis severity subgroups between the three major coronary arteries. Adjusted hazard ratios (aHR) are presented for progression to obstructive CAD among vessels with no or non-obstructive CAD at baseline. The aHR was calculated using a marginal Cox model with the LCx as the reference category. The aHR results were adjusted for the baseline ASCVD risk score, statin use, and per-vessel PAV.

patients experiencing ACS, show the lowest cross-sectional plaque burden in the proximal 30-mm segment of the LCx as compared to its counterpart in the LAD and RCA.[27]

Prior reports are more common among higher risk patients experiencing sudden cardiac death or ACS. Among lower risk cohorts akin to our study, evidence from coronary artery calcium scanning (CACS) reveal the highest scores in the LAD, followed by the RCA and finally the LCx.[28]

Serial evaluation of atherosclerotic plaque progression

A focus of prior series has delineated the steps observed during disease progression culminating in ACS risk or vessel-specific outcome risk.[3,29–31] In contrast, we focus on vessel-specific alterations in atherosclerotic plaque which further modify progressive risk, as noted herein. This study offers novel insights into earlier stages of atherosclerosis as observed in patients undergoing CCTA for evaluation of CAD, as opposed to later stages examined in earlier invasive studies. Similar evidence to date examining atherosclerotic progression is rare but reports similar findings. Interestingly, as atherosclerotic plaque increased, differences between the coronary arteries were minimized. In one report, disease extent was similarly present across the arteries when the total CACS exceeded 1000.[28] We also report no significant differences in atherosclerotic plaque progression between the coronary arteries among patients with obstructive CAD; reinforcing that high-risk disease will beget rapid and more progressive disease states. One additional study examined patients who underwent serial electron-beam tomography noting the lowest annual changes for CACS in the LCx and the greatest changes noted in the LAD.[32] However, among patients with high baseline CACS > 400, progression rates in the LAD were equivalent to those in the LCx. These results align with our report where disease progression equilibrated among patients with obstructive CAD at baseline.

Registry limitations

This study has several limitations. First, only patients undergoing serial CCTA were eligible for enrolment, making selection bias inevitable. The current population is therefore limited to largely low-risk patients. Consequently, the prevalence of cardiovascular events was low, making the study less fit for prognostic analysis. Therefore, the direct association of lower atherosclerotic burden and progression in

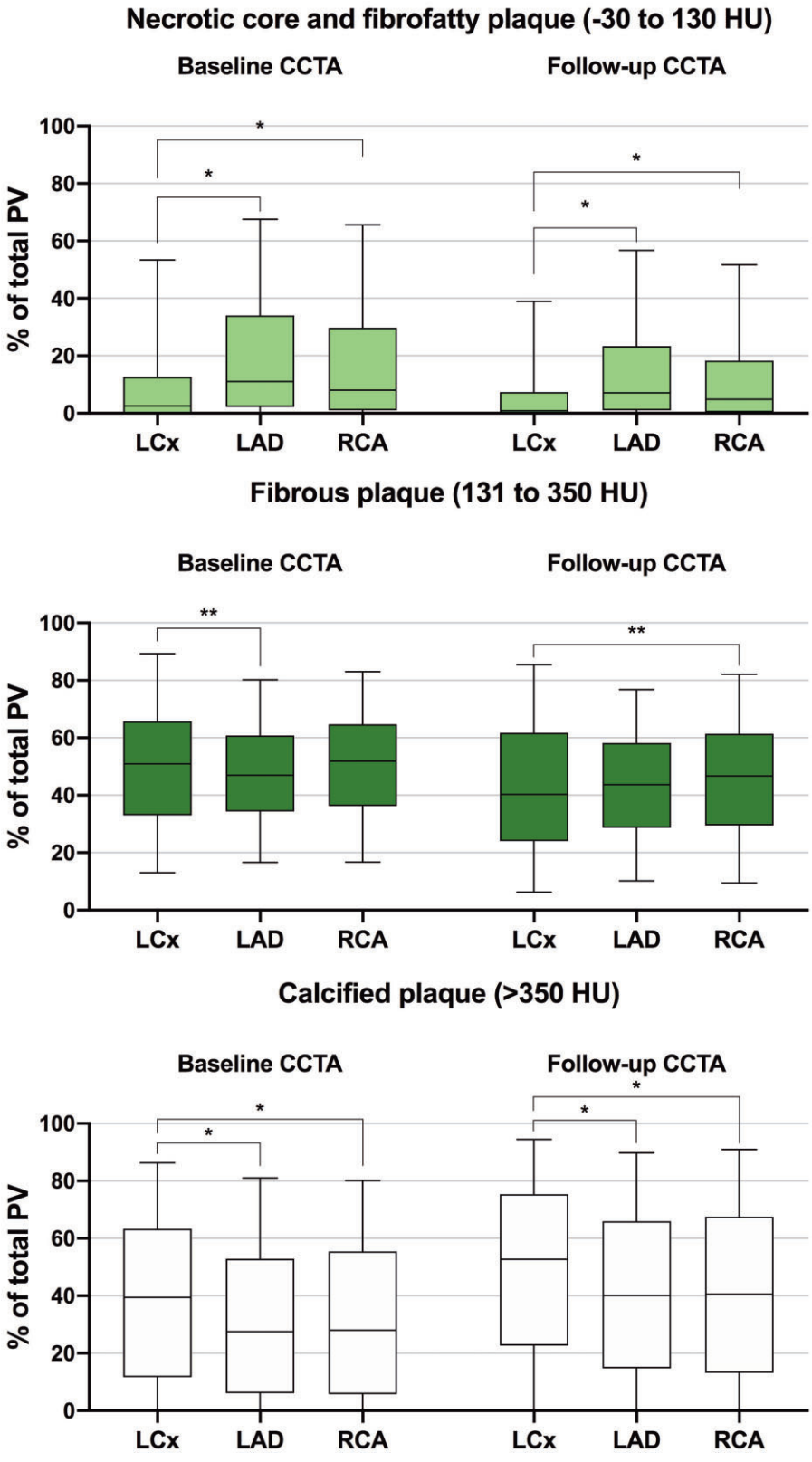

Figure 3 Differences in plaque composition subgroups between the three major coronary arteries at baseline and follow-up. Proportions of total plaque volume (%) are presented for each plaque compositional subtype, in boxplots, representing median with inter-quartile range. Top panel: percentage of necrotic core and fibrofatty plaque (-30 to 130 HU); middle panel: percentage of fibrous plaque (131–350 HU); bottom panel: percentage of calcified plaque (>350 HU). *$P < 0.001$. **$P < 0.05$.

the LCx with the observed lower incidence of MI remains to be investigated. Ideally, our results will be externally validated in large cohorts of varied risk populations. Nevertheless, due to a lack of current recommendations for serial CCTA,[15] the PARADIGM represents the largest available registry for serial CCTA analysis and provides a unique insight into the natural history of atherosclerosis. Secondly, the semiautomated quantification software requires for manual adjustment of centrelines, which is a time-consuming process. Small, tortuous side branches have at times been omitted from quantification.

Conclusions

Our findings reveal novel insights into early patterns of atherosclerotic plaque progression amongst the three major epicardial coronary arteries. Annualized growth in plaque volume and the development of new stenosis occurred less often in the LCx. The patterns of development and progressive alterations within the LCx varied substantially both in terms of types and volumes of change but also in terms of the rate of change, especially when compared with the LAD. These varied patterns of atherosclerotic plaque have marked implications for detection of atherosclerosis and expected patterns of worsening for the symptomatic patient undergoing CCTA.

Supplementary data

Supplementary data are available at *European Heart Journal - Cardiovascular Imaging* online.

Acknowledgements

Dr J.K. Min was involved in this registry prior to leaving Weill Cornell Medical College. He is currently an employee of Cleerly, Inc. He is not listed as an author as he did not contribute to this manuscript, but we acknowledge and are grateful for his contributions to this registry. We thank the PARADIGM investigators for the continued collaboration.

Funding

This work was supported by the Leading Foreign Research Institute Recruitment Program through the National Research Foundation (NRF) of Korea funded by the Ministry of Science and ICT (MSIT) (Grant no. 2012027176). The study was also funded in part by a grant from the Dalio Foundation (New York, NY).

Conflict of interest: K.C. is a non-compensated medical advisor for Heartflow Inc. L.J.S. is on the scientific advisory board for Covanos Inc. J.A.L. is a consultant to and hold stock options in Circle CVI and HeartFlow and receives research support from GE Healthcare and serves on the speakers' bureau for Philips and GE Healthcare. G.S. has received speaker or other honoraria from Cook, Terumo, QOOL Therapeutics, and Orchestra Biomed; has served as a consultant to Valfix, TherOx, Vascular Dynamics, Robocath, HeartFlow, Gore, Ablative Solutions, Miracor, Neovasc, V-Wave, Abiomed, Ancora, MAIA Pharmaceuticals, Vectorious, Reva, Matrizyme, Cardiomech; and has equity/options from Ancora, Qool Therapeutics, Cagent, Applied Therapeutics, Biostar family of funds, SpectraWave, Orchestra Biomed, Aria, Cardiac Success, MedFocus family of funds, and Valfix.

Data availability

The data underlying this article will be shared on reasonable request to the corresponding author.

References

1. Williams MC, Kwiecinski J, Doris M, McElhinney P, D'Souza MS, Cadet S *et al.* Low-attenuation noncalcified plaque on coronary computed tomography angiography predicts myocardial infarction: results from the multicenter SCOT-HEART Trial (Scottish Computed Tomography of the HEART). *Circulation* 2020;**141**:1452–62.
2. Williams MC, Moss AJ, Dweck M, Adamson PD, Alam S, Hunter A *et al.* Coronary artery plaque characteristics associated with adverse outcomes in the SCOT-HEART study. *J Am Coll Cardiol* 2019;**73**:291–301.
3. Chang HJ, Lin FY, Lee SE, Andreini D, Bax J, Cademartiri F *et al.* Coronary atherosclerotic precursors of acute coronary syndromes. *J Am Coll Cardiol* 2018;**71**:2511–22.
4. Ferencik M, Mayrhofer T, Bittner DO, Emami H, Puchner SB, Lu MT *et al.* Use of high-risk coronary atherosclerotic plaque detection for risk stratification of patients with stable chest pain: a secondary analysis of the PROMISE randomized clinical trial. *JAMA Cardiol* 2018;**3**:144–52.
5. Hartmann M, Huisman J, Bose D, Jensen LO, Schoenhagen P, Mintz GS *et al.* Serial intravascular ultrasound assessment of changes in coronary atherosclerotic plaque dimensions and composition: an update. *Eur J Echocardiogr* 2011;**12**:313–21.
6. Bax AM, van Rosendael AR, Ma X, van den Hoogen IJ, Gianni U, Tantawy SW *et al.* Comparative differences in the atherosclerotic disease burden between the epicardial coronary arteries: quantitative plaque analysis on coronary computed tomography angiography. *Eur Heart J Cardiovasc Imaging* 2021;**22**:322–30.
7. Lee SE, Chang HJ, Rizvi A, Hadamitzky M, Kim YJ, Conte E *et al.* Rationale and design of the Progression of AtheRosclerotic PlAque DetermIned by Computed TomoGraphic Angiography IMaging (PARADIGM) registry: a comprehensive exploration of plaque progression and its impact on clinical outcomes from a multicenter serial coronary computed tomographic angiography study. *Am Heart J* 2016;**182**:72–9.
8. Lee SE, Chang HJ, Sung JM, Park HB, Heo R, Rizvi A *et al.* Effects of statins on coronary atherosclerotic plaques: the PARADIGM study. *JACC Cardiovasc Imaging* 2018;**11**:1475–84.
9. Abbara S, Blanke P, Maroules CD, Cheezum M, Choi AD, Han BK *et al.* SCCT guidelines for the performance and acquisition of coronary computed tomographic angiography: a report of the society of Cardiovascular Computed Tomography Guidelines Committee: endorsed by the North American Society for Cardiovascular Imaging (NASCI). *J Cardiovasc Comput Tomogr* 2016;**10**:435–49.
10. Park HB, Lee BK, Shin S, Heo R, Arsanjani R, Kitslaar PH *et al.* Clinical feasibility of 3D automated coronary atherosclerotic plaque quantification algorithm on coronary computed tomography angiography: comparison with intravascular ultrasound. *Eur Radiol* 2015;**25**:3073–83.
11. Leipsic J, Abbara S, Achenbach S, Cury R, Earls JP, Mancini GJ *et al.* SCCT guidelines for the interpretation and reporting of coronary CT angiography: a report of the Society of Cardiovascular Computed Tomography Guidelines Committee. *J Cardiovasc Comput Tomogr* 2014;**8**:342–58.
12. de Graaf MA, Broersen A, Kitslaar PH, Roos CJ, Dijkstra J, Lelieveldt BP *et al.* Automatic quantification and characterization of coronary atherosclerosis with computed tomography coronary angiography: cross-correlation with intravascular ultrasound virtual histology. *Int J Cardiovasc Imaging* 2013;**29**:1177–90.
13. Achenbach S, Moselewski F, Ropers D, Ferencik M, Hoffmann U, MacNeill B *et al.* Detection of calcified and noncalcified coronary atherosclerotic plaque by contrast-enhanced, submillimeter multidetector spiral computed tomography: a segment-based comparison with intravascular ultrasound. *Circulation* 2004;**109**:14–7.
14. van Rosendael AR, Lin FY, Ma X, van den Hoogen IJ, Gianni U, Al Hussein O *et al.* Percent atheroma volume: optimal variable to report whole-heart atherosclerotic plaque burden with coronary CTA, the PARADIGM study. *J Cardiovasc Comput Tomogr* 2020;**14**:400–6.
15. Task Force M, Montalescot G, Sechtem U, Achenbach S, Andreotti F, Arden C *et al.* ESC guidelines on the management of stable coronary artery disease: the Task Force on the management of stable coronary artery disease of the European Society of Cardiology. *Eur Heart J* 2013;**34**:2949–3003. 2013;
16. Puchner SB, Liu T, Mayrhofer T, Truong QA, Lee H, Fleg JL *et al.* High-risk plaque detected on coronary CT angiography predicts acute coronary syndromes independent of significant stenosis in acute chest pain: results from the ROMICAT-II trial. *J Am Coll Cardiol* 2014;**64**:684–92.
17. Motoyama S, Ito H, Sarai M, Kondo T, Kawai H, Nagahara Y *et al.* Plaque characterization by coronary computed tomography angiography and the likelihood of acute coronary events in mid-term follow-up. *J Am Coll Cardiol* 2015;**66**:337–46.

18. Lee SE, Sung JM, Rizvi A, Lin FY, Kumar A, Hadamitzky M *et al.* Quantification of coronary atherosclerosis in the assessment of coronary artery disease. *Circ Cardiovasc Imaging* 2018;**11**:e007562.
19. Han D, Kolli KK, Al'Aref SJ, Baskaran L, van Rosendael AR, Gransar H *et al.* Machine learning framework to identify individuals at risk of rapid progression of coronary atherosclerosis: from the PARADIGM Registry. *J Am Heart Assoc* 2020; **9**:e013958.
20. Budoff MJ, Mayrhofer T, Ferencik M, Bittner D, Lee KL, Lu MT *et al.* Prognostic value of coronary artery calcium in the PROMISE Study (Prospective Multicenter Imaging Study for Evaluation of Chest Pain). *Circulation* 2017;**136**: 1993–2005.
21. van Rosendael AR, Shaw LJ, Xie JX, Dimitriu-Leen AC, Smit JM, Scholte AJ *et al.* Superior risk stratification with coronary computed tomography angiography using a comprehensive atherosclerotic risk score. *JACC Cardiovasc Imaging* 2019;**12**:1987–97.
22. Stone PH, Maehara A, Coskun AU, Maynard CC, Zaromytidou M, Siasos G *et al.* Role of low endothelial shear stress and plaque characteristics in the prediction of nonculprit major adverse cardiac events: the PROSPECT Study. *JACC Cardiovasc Imaging* 2018;**11**:462–71.
23. Samady H, Eshtehardi P, McDaniel MC, Suo J, Dhawan SS, Maynard C *et al.* Coronary artery wall shear stress is associated with progression and transformation of atherosclerotic plaque and arterial remodeling in patients with coronary artery disease. *Circulation* 2011;**124**:779–88.
24. Montenegro MR, Eggen DA. Topography of atherosclerosis in the coronary arteries. *Lab Invest* 1968;**18**:586–93.
25. White NK, Edwards JE, Dry TJ. The relationship of the degree of coronary atherosclerosis with age, in men. *Circulation* 1950;**1**:645–54.
26. Virmani RENU, Burke AP, Kolodgie FD, Farb A. of the thin-cap fibroatheroma: a type of vulnerable plaque. *J Interv Cardiol* 2003;**16**:267–72.
27. Wykrzykowska JJ, Mintz GS, Garcia-Garcia HM, Maehara A, Fahy M, Xu K *et al.* Longitudinal distribution of plaque burden and necrotic core-rich plaques in nonculprit lesions of patients presenting with acute coronary syndromes. *JACC Cardiovasc Imaging* 2012;**5**:S10–8.
28. Iwasaki K, Matsumoto T, Aono H, Furukawa H, Nagamachi K, Samukawa M. Distribution of coronary atherosclerosis in patients with coronary artery disease. *Heart Vessels* 2010;**25**:14–8.
29. Ahmadi A, Leipsic J, Blankstein R, Taylor C, Hecht H, Stone GW *et al.* Do plaques rapidly progress prior to myocardial infarction? The interplay between plaque vulnerability and progression. *Circ Res* 2015;**117**:99–104.
30. Stone GW, Maehara A, Lansky AJ, de Bruyne B, Cristea E, Mintz GS *et al.* A prospective natural-history study of coronary atherosclerosis. *N Engl J Med* 2011; **364**:226–35.
31. Ahmadi A, Argulian E, Leipsic J, Newby DE, Narula J. From subclinical atherosclerosis to plaque progression and acute coronary events: JACC state-of-the-art review. *J Am Coll Cardiol* 2019;**74**:1608–17.
32. Schmermund A, Baumgart D, MöHlenkamp S, Kriener P, Pump H, GröNemeyer D *et al.* Natural history and topographic pattern of progression of coronary calcification in symptomatic patients: an electron-beam CT study. *ATVB* 2001;**21**: 421–6.